COMPARISON BETWEEN THE DOUBLE-*K* FRACTURE MODEL AND THE TWO PARAMETER FRACTURE MODEL

VERGLEICH ZWISCHEN DEM DOPPEL-K-BRUCHMODELL UND DEM ZWEIPARAMETERBRUCHMODELL

COMPARAISON ENTRE LE MODELE DE FRACTURE DOUBLE-K ET LE MODELE DE RUPTURE DEUX PARAMETRES

Shilang Xu[1,2], Hans W. Reinhardt[2], Zhimin Wu[1] and Yanhua Zhao[1]

1 Department of Civil Engineering, Dalian University of Technology, Dalain, China

2 Institute of Construction Materials, University of Stuttgart, Stuttgart, Germany

ABSTRACT

Concrete fracture experiments on both the three-point bending notched beams and the wedge splitting specimens with different relative initial crack length (a_0/D) were carried out according to the experimental requirements for determining the fracture parameters introduced in the Double-*K* Fracture Model (DKFM) proposed by Xu and Reinhardt in recent years and the Two Parameter Fracture Model (TPFM) proposed by Jenq and Shah in 1985. The results of the comparison showed that the critical crack length a_c determined using the two different models are hardly different. The values of K_{Ic}^{un} and $CTOD_c$ measured for the DKFM are in good agreement with K_{Ic}^{s} and $CTOD_c$ measured for the TPFM.

However, the testing procedure of the TPFM needs a closed-loop testing machine whereas the DKFM needs only monotonic loading. In the TPFM a high order nonlinear equation has to be solved in order to get the relevant parameters whereas in the DKFM the parameters can be determined analytically on a pocket calculator. Furthermore, the DKFM supplies more information on the fracture process.

ZUSAMMENFASSUNG

Betonbruchversuche an gekerbten Dreipunktbiegebalken und Keilspaltenproben mit unterschiedlicher Anfangsrisslänge (a_0/D) wurden durchgeführt, wobei die Versuchsbedingungen zur Bestimmung der Bruchparameter entsprechend dem Doppel-K-Bruchmodell (DKFM), kürzlich vorgeschlagen von Xu und Reinhardt, und dem Zweiparameterbruchmodell (TPFM), 1985 vorgeschlagen von Jeng und Shah, eingehalten wurden. Die Ergebnisse des Vergleichs zeigten, dass sich die kritische Risslänge a_c nach den zwei Modellen kaum unterscheidet. Die Werte von K_{Ic}^{un} und $CTOD_c$, gemessen für das TPFM, sind in guter Übereinstimmung mit K_{Ic}^{s} und $CTOD_c$ nach dem DKFM.

Die Versuchsdurchführung des TPFM benötigt indessen eine verformungsgesteuerte Prüfmaschine, während beim DKFM monotone Belastung ausreicht. Im TPFM muss eine nichtlineare Gleichung höherer Ordnung gelöst werden, um die maßgeblichen Bruchparameter zu bekommen, während diese im DKFM analytisch mit einem Taschenrechner bestimmt werden können. Außerdem enthält das DKFM mehr Information über den Bruchprozess.

RESUME

Des essais de rupture de béton ont été réalisés par flexion trois points sur des éprouvettes entaillées et par partage en biseau. Ces essais ont été réalisés pour des longueurs de fentes initiales (a_0/D) variables selon les exigences expérimentales pour la détermination des paramètres de rupture introduits dans le modèle de rupture double-K (DKFM) proposé récemment par Xu et Reinhardt et le modèle de rupture deux paramètres (TPFM) proposé par Jenq et Shah en 1985. Les résultats montrent que les longueurs de la fente critique a_c déterminées pour les deux modèles ne diffèrent guère. Les valeurs de K_{Ic}^{un} et $CTOD_c$ mesurées pour le DKFM correspond bien avec les valeurs de K_{Ic}^{s} et $CTOD_c$ mesurées pour le TPFM.

Cependant la procédure d'essai du TPFM requiert une machine à contrôle en boucle fermée, tandis qu'un chargement monotone suffit pour le DKFM. Pour le TPFM, une équation non-linéaire de haut ordre doit être résolue afin de déterminer les paramètres centraux, tandis que les paramètres du DKFM peuvent être déterminés analytiquement sur une calculatrice de poche. En outre, le DKFM livre plus d'informations sur le processus de rupture.

1 INTRODUCTION

Past attempts at describing the fracture behavior of concrete from the standpoint of conventional linear elastic fracture mechanic (LEFM) have not been very successful, because of the existence of the fracture process zone (FPZ) and the cohesive force ahead of a traction-free crack. In order to predict the crack propagation and to reflect the effluence of the FPZ on the fracture characteristic of materials, several fracture models, like the fictitious crack model (FCM) by Hillerborg et al. (1976), the crack band model (CBM) by Bazant and Oh (1983), the two parameter fracture model (TPFM) by Jenq and Shah (1985), the effective crack model (ECM) by Karihaloo and Nallathambi (1990) and Swartz and Refai (1987) as well as the size effect model (SEM) by Bazant, Kim and Pfeiffer (1986) have been presented. Based on different hypothesis and explanation for the phenomenon of non-linearity observed in tests, many of these models introduced the modified fracture parameters to predict the fracture behavior of concrete structures still by applying the conventional LEFM.

Typical among aforementioned models is TPFM. In the TPFM, two fracture parameters are proposed, namely the critical stress intensity factor K_{Ic}^{s} defined as the stress intensity factor calculated at the critical effective crack tip and the critical crack tip opening displacement $CTOD_c$ defined as the crack tip opening displacement calculated at the original notch tip of the specimen. For determining them, an unloading and reloading procedure is needed to be performed in tests so that an unloading compliance c_u can be used to evaluated the effective crack length a_c. Then the measured value of the peak load $P_{\max}$ and the evaluated value of the effective crack length a_c are inserted into a formula of LEFM to determine K_{Ic}^{s} and $CTOD_c$.

In recent decades, more and more experimental investigations have showed that the fracture process in concrete structures includes three manifest stages: crack initiation, stable crack propagation and unstable fracture (or failure). So it is hoped that any fracture model could be depict these three stages in crack propagation. While all the above-mentioned fracture models can only be used to predict the unstable fracture of concrete structures without considering the crack initiation. For a normal structure, it may be sufficient only to predict its failure or unstable fracture under given loading or displacement conditions accurately. But for some special and important structures, for example, for a concrete pressure vessel or a high concrete dam, accurate prediction of both failure and crack

initiation are imperative. In some cases, accurate prediction of the crack initiation is more important. In engineering practice, one may expect a fracture model is not only accurate for predicting the behavior of cracked structures, but also simple for evaluating the corresponding fracture parameters introduced in the model. Therefore an analytical fracture model that can contain these three stages and also easy to be conducted in tests is required for practical purpose.

In order to reflect the different stages in concrete fracture, a double-*K* fracture criterion is proposed by Shilang Xu and Reinhardt (1999a). In the double-*K* fracture criterion, the two fracture parameters (K_{Ic}^{ini} and K_{Ic}^{un}) are introduced, both of them are given in terms of stress intensity factor. K_{Ic}^{ini} is called the initiation toughness and its value is determined by inserting the initial cracking load P_{ini} and the initial crack length a_0 into a formula of LEFM. K_{Ic}^{un} is termed the unstable fracture toughness or the critical stress intensity factor and its value is determined by inserting the measured maximum load $P_{\max}$ and the measured critical effective crack length a_c into the same formula of LEFM. It is found that K_{Ic}^{ini} and K_{Ic}^{un} are size-independent for the tested specimens. Also, for determining the double-*K* parameters, there is no need to unloading and reloading procedure, and a closed-loop system is not necessary.

In this report, a detailed comparison between the double-*K* model and the TPFM is made to clearly see the main difference between them and well understanding the effect of FPZ and cohesive force on the fracture characteristic of concrete material.

2 THE COMPARISON IN THEORY AND EXPERIMENT METHOD BETWEEN THE DOUBLE-*K* CRITERION AND TPFM

A load-*CMOD* (crack mouth opening displacement) plot of a typical pre-notched beam tested in three-point bending is shown in Fig. 1. The nonlinear displacement can be attributed to the slow but stable crack growth preceding the attainment of the peak load. The effective crack length a_c, the sum of the initial crack length a_0 plus the stable crack growth Δa_c is corresponding to the maximum load $P_{\max}$. While in the reasonable evaluation of the effective crack length a_{c}, the TPFM and the double-*K* are based on the different hypothesis and theory concept. In the TPFM it is considered that the nonlinearity segment on the *P*-*CMOD* is mainly due to the elastic $CMOD_{\mathrm{n}}^{e}$ and only the elastic part $CMOD^{e}$ or the compliance C_{u} measured on the unloading line AA^{1} is taking into account to

calculate the effective crack length a_c. While it may be lead to an underestimate of the a_c, because the nonlinear behavior in the *P-CMOD* plot results from both the residual $CMOD^p$ that the plastic-frictional energy dissipated on it cannot be neglected (Bazant, 1996) and the $CMOD_n^e$, the difference between the initial elastic compliance C_i and the unloading elastic compliance C_u. So in the double-*K* , based on the linear asymptotic superposition, the scant compliance c_s as illustrated in Fig. 1, or $CMOD_c$ (including the elastic part $CMOD^e$ and the unrecoverable deformation $CMOD^p$), is used to calculate the effective crack length a_c, which consists of an equivalent-elastic stress-free crack and an equivalent-elastic fictitious crack extension.

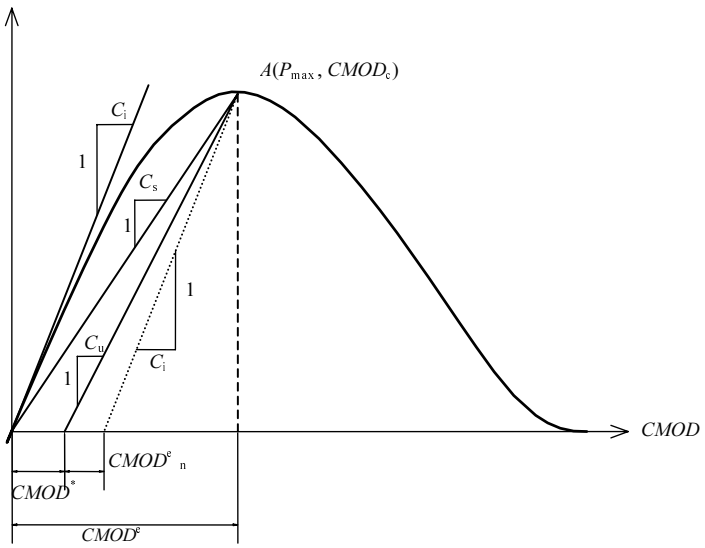

*Fig. 1 A load-*CMOD *curve tested on the three-point bending beam*

Another difference between these two models lies in the selection of fracture parameters. As above-mentioned, the TPFM choose the critical stress intensity factor K_{Ic}^s, similar to unstable fracture toughness K_{Ic}^{un} in double-*K* , it can predict the unstable fracture of concrete structures. But, this model cannot be used to depict the crack initiation which has been observed by many researchers with different investigating methods. Therefore, for some special cases the applications of this model are somewhat restricted. Yet, in the double-*K* , the initiation fracture toughness K_{Ic}^{ini} is also introduced to represent the onset of stable crack propagation. Besides, these two fracture toughness are not isolated, the

difference is the cohesion toughness K_{Ic}^{c} due to cohesive forces distributed on the fictitious crack during crack propagation. Their relationship is as follows (Shilang Xu and Reinhardt, 1999b):

$$K_{Ic}^{ini} = K_{Ic}^{un} - K_{Ic}^{c} \tag{1}$$

The dissimilarity in the explanation of cause of non linear feature in *P-CMOD* curve leads to the difference in test methods. In the TPFM, unloading compliance C_u is needed to calculate the effective crack length a_c , so at least one unloading and reloading procedure should be carried out, and for achieving the stable unloading after the maximum load, a closed-loop testing system is necessary. However some advantages in the TPFM are favourable. For example, only a single size of three-point bend beams is needed in the tests, all of fracture parameters, like K_{Ic}^{s} , $CTOD_c$, a_c can be directly measured. So it is possible that the properties of size-independence of K_{Ic}^{s} and $CTOD_c$ claimed by Jenq and Shah (1985) which are evaluated by the method described in (Jenq and Shah, 1985: RILEM, 1990) could be further justified by the results that are directly measured. In double-K , for the mensuration of the double-K fracture parameters, K_{Ic}^{ini} and K_{Ic}^{un} , tests on a single size of three-point bending notched beams are needed. The testing procedure is rather simple without unloading and reloading procedures. It only needs to apply monotonously a load on a beam until the maximum load is gained and to measure the rising branch of a *P-CMOD* curve. For achieving such an aim to measure the initial compliance c_i and the c_s in tests, a closed-loop testing system is not necessary.

3 TEST RESULTS AND CALCULATIONS

Because the main difference is the evaluation of effective crack length a_c owning to the different explanation of non-linear segment in a *P-CMOD* plot, so the emphasis is focused on the calculation of a_c. Tests to determine the fracture parameters are performed on two groups specimens, standard three-point bending notched beams denoted with serials B and the wedging splitting specimens represented by serials WS. For these two groups, the cubical compressive strength f_{cu} is 47.96 MPa, and the maximum size of the coarse aggregate is 20 mm, and the static dead load for specimens is 24 KN/m^3, and the self weight of loading facilities is 0.23 KN.

The configuration of three-point bending notched beam (BM) and wedging splitting specimens (WS) are illustrated in fig. 2. The dimensions for series BM are 800×200×200 (span×depth×thickness) with ratio of the initial crack length a_0 against D as the variable, and series WS with dimensions 200×200×200 (D_1×H×B). During tests, load is measured through a sensor and a clip gauge is employed to record the crack mouth opening displacement *CMOD*, and these data are picked continuously through "GRAB" picking system. The test results in terms of *P*-*CMOD* for BM (or P_v-*CMOD* for WS) curve is shown in fig. 3 and fig. 4, and the measured results like the peak load P_{max} for BM (or P_{vmax}, for WS) the $CMOD_c$, the initial compliance C_i , the scant compliance C_s, as well as unloading C_u are listed in Table 1 and Table 2. With these directly measured data, fracture parameters such as the critical stress intensity factor K_{Ic}^{s} the critical crack tip opening displacement $CTOD_c$ in TPFM, K_{Ic}^{ini} and K_{Ic}^{un} in the double-*K* , and the effective crack length a_c can all be determined.

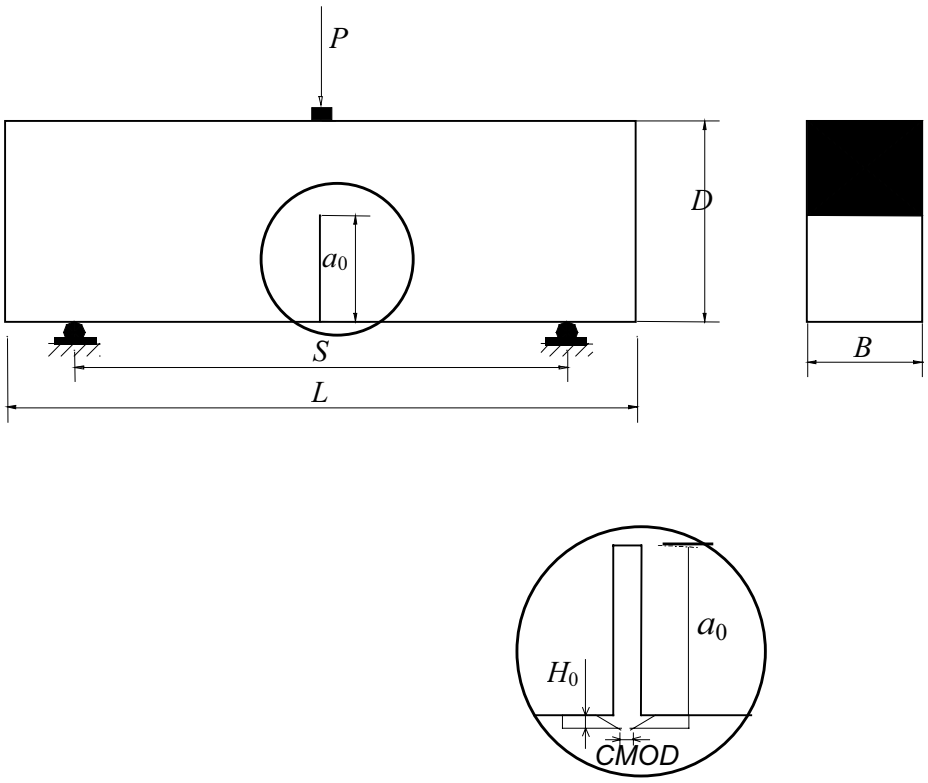

Fig. 2 (a) the configuration of three-point bending beam (BM)

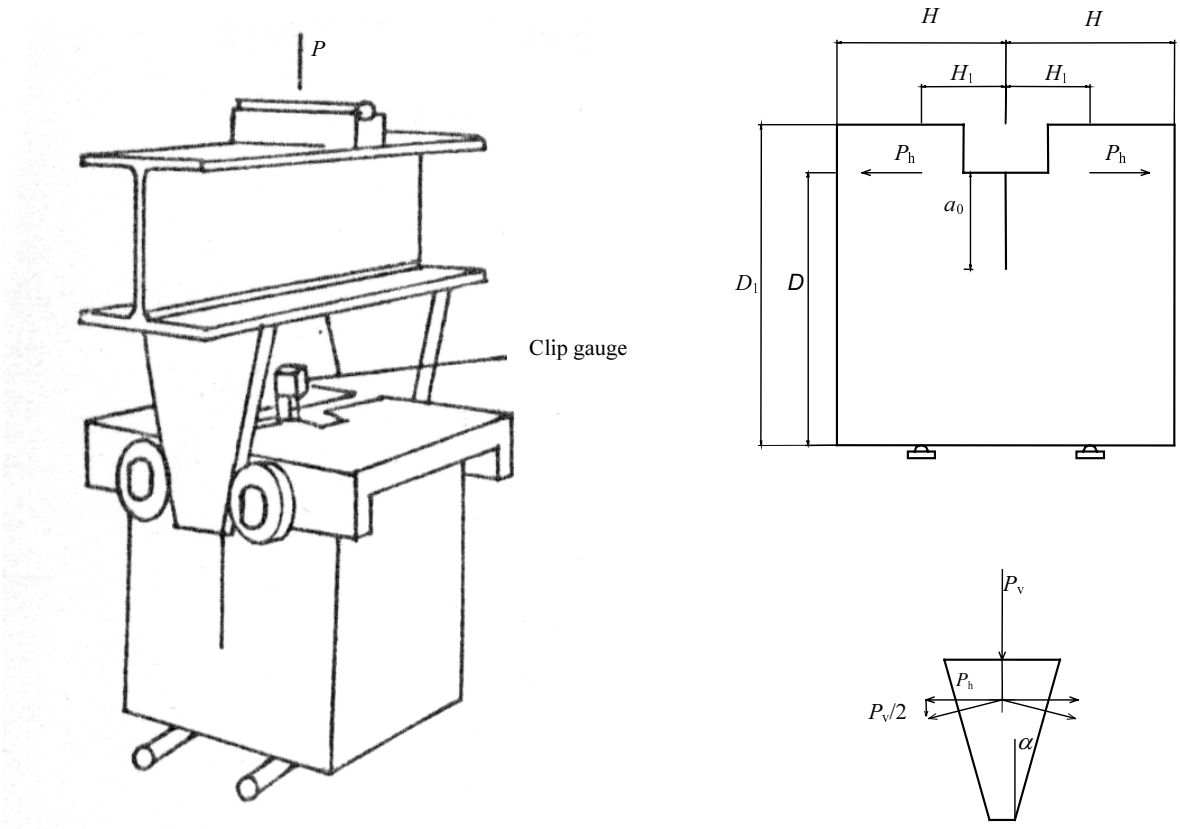

Fig. 2 (b) the configuration of wedge splitting specimen (WS)

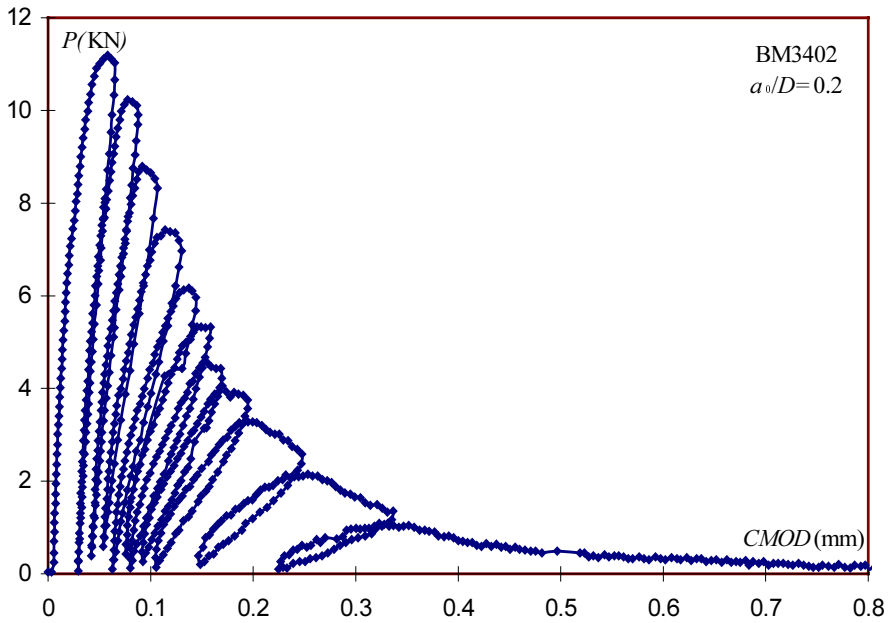

Fig. 3 (a) $a_0/D=0.2$

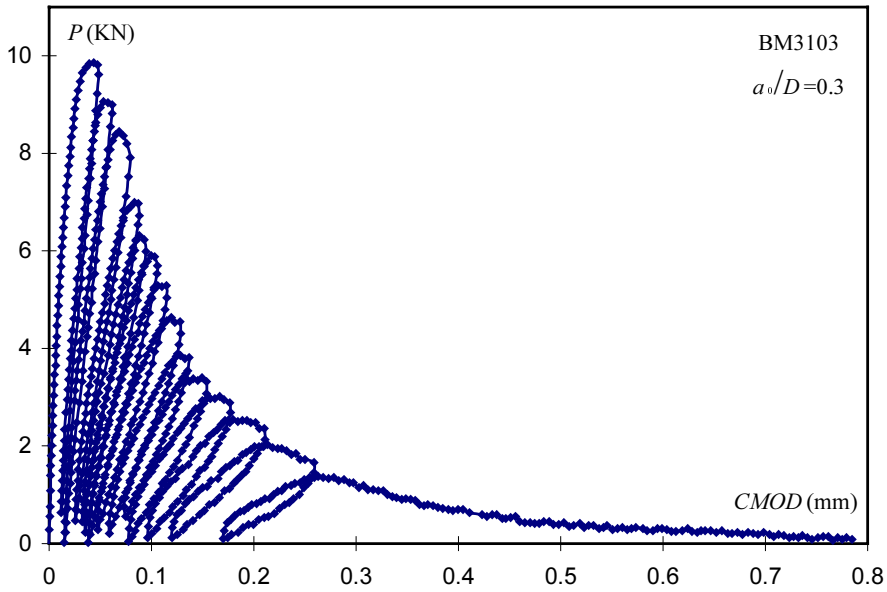

Fig. 3 (b) $a_0/D=0.3$

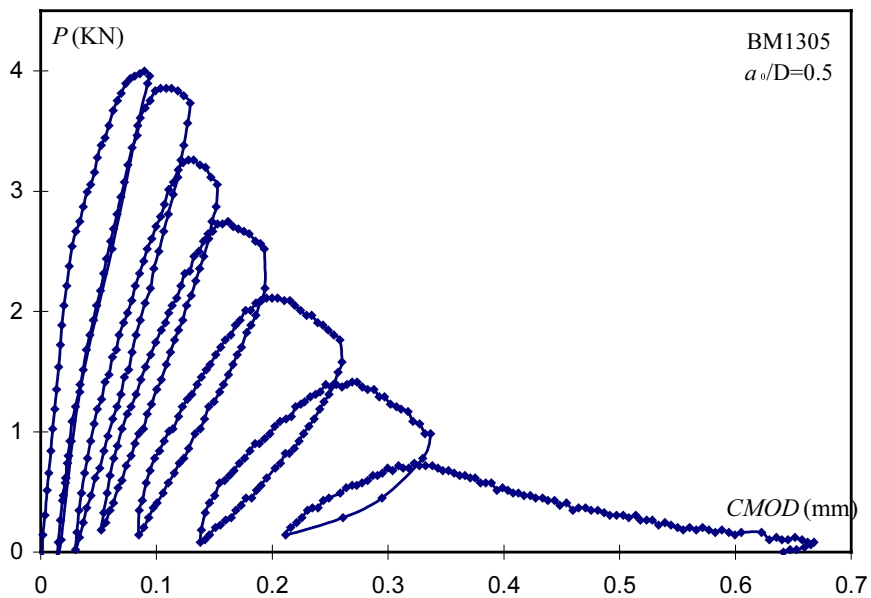

Fig. 3 (c) $a_0/D=0.5$

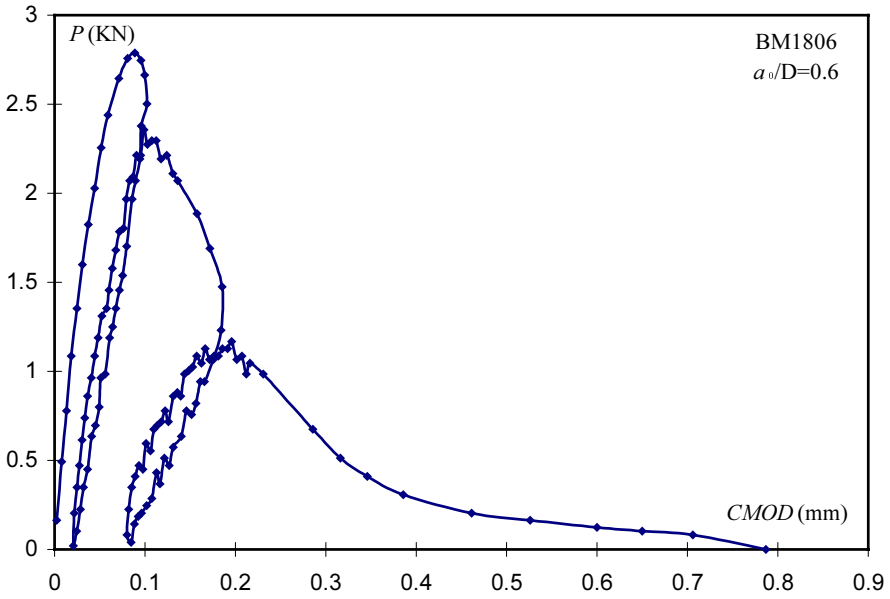

Fig. 3 (d) $a_0/D=0.6$

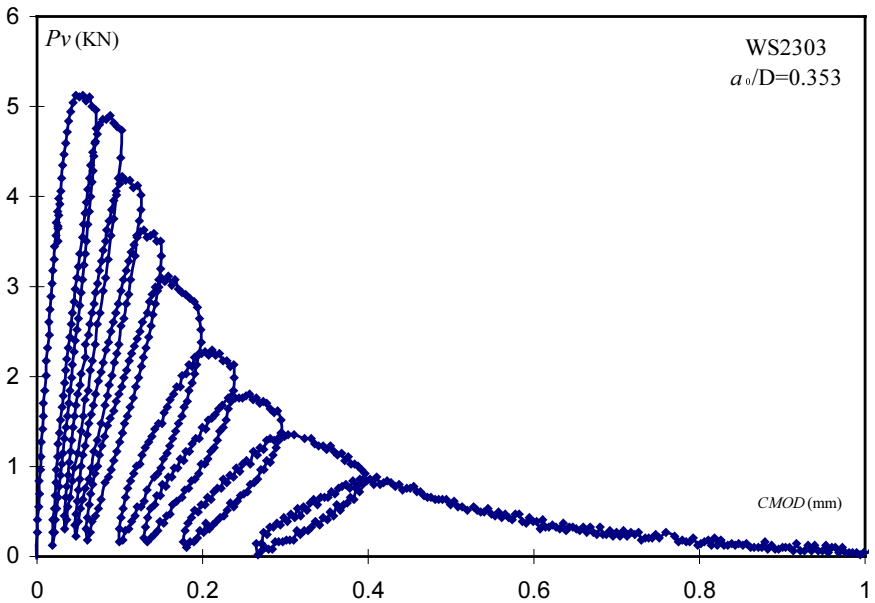

Fig. 4 (a) $a_0/D=0.353$

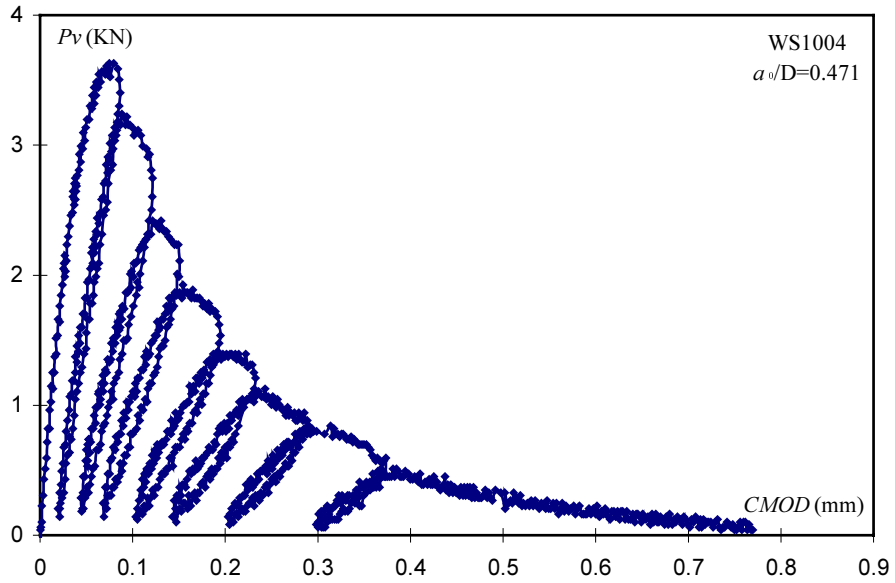

Fig. 4 (b) $a_0/D=0.471$

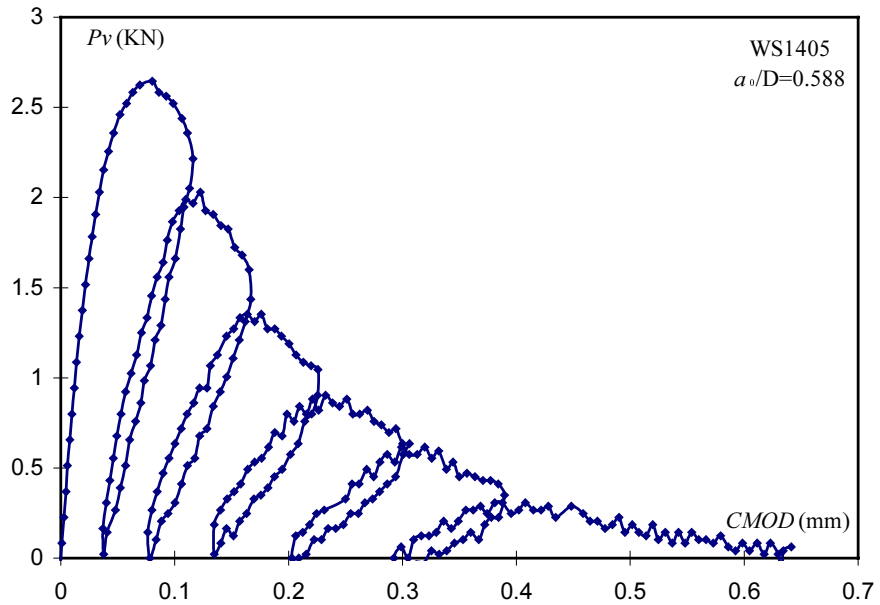

Fig. 4 (c) $a_0/D=0.588$

WS2606
a_0/D=0.706

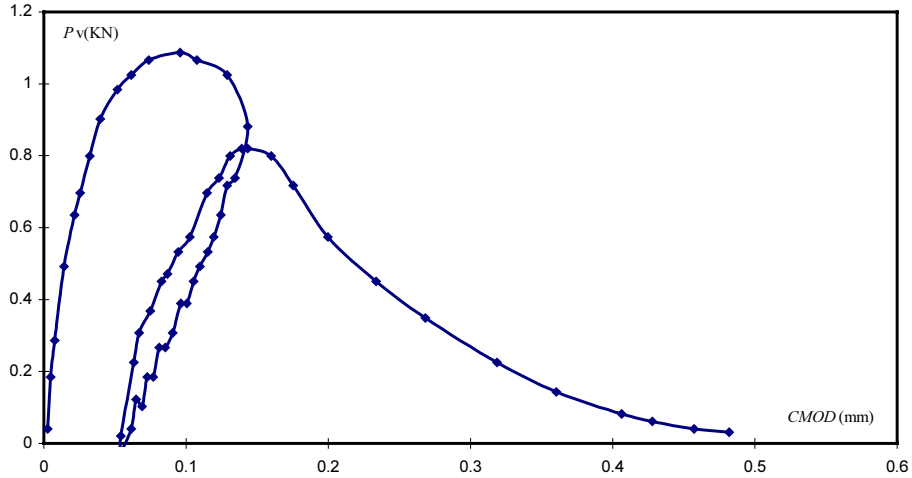

Fig 4. (d) $a_0/D=0.706$

*Table 1 The measured results of series BM specimens (*S×D×B=*800×200×200mm,* H_0=*1mm,* f_{cu}=*47.96MPa)*

Nos. of Specs.	a_0/D	P_{max} (KN)	$CMOD_c$(mm)	C_ix10^{-3} (mm/KN)	C_sx10^{-3} (mm/KN)	C_ux10^{-3} (mm/KN)
BM102	0.2	11.1	0.045	1.872	4.054	
BM402	0.2	8.9585	0.03	1.933	3.349	
BM3402	0.2	11.193	0.0579	2.074	5.173	3.255
BM3502	0.2	10.004	0.0498	1.924	4.978	
BM3602	0.2	10.66	0.0417	2.408	3.912	4.177
BM303	0.3	8.282	0.0543	3.686	6.556	
BM2603	0.3	7.872	0.0546	3.972	6.936	8.013
BM2703	0.3	9.922	0.0642	3.553	6.470	6.392
BM2803	0.3	7.831	0.0552	3.625	7.049	
BM2903	0.3	7.79	0.0585	3.723	7.510	8.706
BM3003	0.3	7.38	0.0543	3.377	7.358	6.606
BM705	0.5	5.6375	0.084	10.976	14.900	
BM805	0.5	3.9565	0.0717	12.274	18.122	
BM1205	0.5	3.5055	0.0642	8.595	18.314	
BM1305	0.5	3.9975	0.0897	9.469	22.439	19.935
BM1505	0.5	4.674	0.0645	8.564	13.800	
BM2005	0.5	4.8585	0.069	9.690	14.202	13.940
BM1406	0.6	1.7015	0.0837	17.960	49.192	
BM1806	0.6	2.788	0.0888	16.543	31.851	29.869
BM1906	0.6	1.517	0.0528	14.939	34.806	

Table 2 The measured results of series WS specimens ($D_1 \times H \times B = 200 \times 200 \times 200mm$, $H_0 = 1mm$, $f_{cu} = 47.96MPa$)

Nos. of Specs.	a_0/D	P_{vmax} (KN)	$CMOD_c$(mm)	$C_{sv}x10^{-3}$ (mm/KN)	$C_{iv}x10^{-3}$ (mm/KN)	$C_{uv}x10^{-3}$ (mm/KN)
WS102	0.235	9.799	0.0648	6.613	2.796	6.436
WS2902	0.235	6.847	0.0459	6.704	2.832	5.618
WS1803	0.353	5.7195	0.0624	10.910	4.878	
WS2103	0.353	6.806	0.0675	9.918	4.823	8.212
WS2203	0.353	5.74	0.0663	11.551	4.760	10.591
WS2303	0.353	5.125	0.0552	10.771	4.814	10.852
WS2403	0.353	5.904	0.0588	9.959	4.257	9.113
WS2703	0.353	6.0887	0.0627	10.298	4.768	9.589
WS2803	0.353	5.8835	0.0675	11.473	4.756	
WS604	0.471	3.485	0.0564	16.184	8.574	
WS704	0.471	4.4075	0.0669	15.179	7.792	15.751
WS904	0.471	3.567	0.0744	20.858	9.083	19.319
WS1004	0.471	3.6285	0.0795	21.910	9.756	19.185
WS1104	0.471	3.731	0.0699	18.735	8.272	17.271
WS1205	0.588	2.1935	0.0576	26.259	15.236	24.191
WS1305	0.588	2.337	0.0741	31.707	15.277	25.849
WS1405	0.588	2.6445	0.0804	30.403	15.475	24.470
WS1505	0.588	2.132	0.0804	37.711	15.284	33.001
WS1605	0.588	2.3985	0.0798	33.271	14.891	28.320
WS1705	0.588	2.6445	0.0861	32.558	15.549	23.914
WS2005	0.588	2.583	0.0675	26.132	15.512	22.671
WS2506	0.706	1.353	0.1044	77.162	33.551	53.078
WS2606	0.706	1.0865	0.0957	88.081	33.989	71.736
WS3006	0.706	1.3735	0.093	67.710	32.999	55.335
WS3106	0.706	1.2915	0.0699	54.123	33.592	42.759

Then, the necessary equations for the calculation of fracture parameters for series BM and WS specimens will be detailed subsequently.

THE CALCULATIONS EQUATIONS FOR BM

First, the Young'modulus E can be calculated from the measured initial compliance c_i of *P-CMOD* curve as follows (RILEM, 1990):

$$E = 6Sa_0V_1(\alpha_0)/\left[C_iD^2B\right] \tag{2}$$

for S/D=4, the function $V_1(\alpha_0)$ is given by

$$V_1(\alpha_0) = 0.76 - 2.28\alpha_0 + 3.87\alpha_0^2 - 2.04\alpha_0^3 + 0.66/(1-\alpha_0)^2 \tag{3}$$

where

a_0 = initial crack length;

$\alpha_0 = (a_0+H_0)/(D+H_0)$;

H_0 = thickness of clip gauge holder;

S = specimen loading span;

D = beam depth;

B = beam width;

C_i = the initial compliance from *P-CMOD* curve.

In this step, the TPFM and the double-K is the same, the main difference lies in the determination of the effective crack length, Based on the linear asymptotic superposition assumption, the double-K solves the effective crack length denoted by a_{ck} by LEFM as follows (Tada, 1985):

$$E = 6Sa_cV_1(\alpha_c)/\left[C_sD^2B\right] \tag{4}$$

where

a_c = critical effective crack length to be determined;

$\alpha_c = (a_c+H_0)/(D+H_0)$;

C_s = the scant compliance from *P-CMOD* curve , equal to $CMOD_c/P_{max}$.

While, in the TPFM, the effective crack length denoted by a_{cp} is calculated from the unloading compliance C_u at 95% of peak load, so substitute C_u for C_s in equation (4), the a_{cp} described in the TPFM can be got. The comparison of a_{ck} and a_{cp} is listed in table 3.

*Table 3 the comparison of the TPFM and the double-*K *model in terms of effective crack length for BM specimens*

No.	a_0/D	C_ix10^{-3} (mm/KN)	C_sx10^{-3} (mm/KN)	C_ux10^{-3} (mm/KN)	E(Mpa)	a_{ck}/D	a_{cp}/D
BM3402	0.2	2.074	5.173	3.255	34255	0.279	0.368
BM3602	0.2	2.408	3.912	4.177	29500	0.298	0.286
BM2603	0.3	3.972	6.936	8.013	31320	0.434	0.406
BM2703	0.3	3.553	6.470	6.392	35010	0.412	0.414
BM2903	0.3	3.723	7.510	8.706	33420	0.461	0.434
BM3003	0.3	3.377	7.358	6.606	36840	0.428	0.448
BM1305	0.5	9.469	22.439	19.935	38010	0.624	0.642
BM2005	0.5	9.690	14.202	13.940	37140	0.563	0.566
BM1806	0.6	16.543	31.851	29.869	39270	0.686	0.695

After the effective crack length is known, the fracture toughness K_{Ic}^{ini} and K_{Ic}^{un} can be decided. As previous stated, the unstable fracture toughness K_{Ic}^{un} is corresponding to (P_{max} , a_{ck}), so it can be evaluated by inserting the maximum load P_{max} and the critical crack length a_{ck} into the following expression (Tada et al., 1985):

$$K_{Ic}^{un} = 3(P_{max} + 0.5W)SF_1(\alpha_{ck}) \big/ (2D^2B) \tag{5}$$

in which

$$F_1(\alpha_{ck}) = \frac{1.99 - \alpha_{ck}(1-\alpha_{ck})(2.15 - 3.93\alpha_{ck} + 2.7\alpha_{ck}^{\ 2})}{(1+2\alpha_{ck})(1-\alpha_{ck})^{3/2}} \tag{6}$$

where

$\alpha_{ck} = a_{ck}/D$;

$W = W_0 S/L$, and W_0 is the self weight of the beam.

As for the initial fracture toughness K_{Ic}^{ini}, it will be calculated based on the equation (1), and the details of analytical solution for K_{Ic}^{c} caused by the cohesive force is presented in (Shilang Xu and Reinhardt, 2000), herein it is briefed for the completeness of the report.

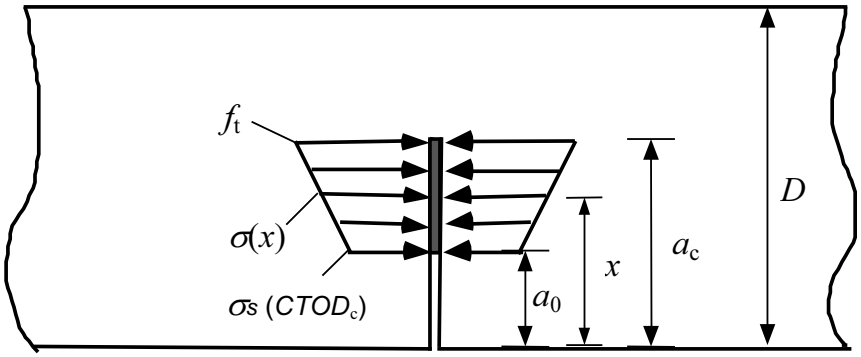

Fig. 5 The calculation figure of the cohesive fracture toughness K_{Ic}^{c}

As shown in Fig. 5, the distributed cohesive force σ(x) is replaced by a concentrated load P_e , acting on the centroid of the cohesive force σ(x), and the equation for K_{Ic}^{c} can be written as (let $\beta=\sigma_s(CTOD)/f_t$, $V_0=a_0/D$, $V_c = a_{ck}/D$, $U_e =x_e/a_{ck}$, x_e is the distance of the acting point of P_e from the bottom of the beam):

$$K_{Ic}^{c}/\, f_t\sqrt{D} = \frac{2P_e}{f_t\sqrt{\pi\, a_{ck} D}} Z(U_e, V_0/V_c)\, F(U_e, V_c) = (1+\beta)\sqrt{V_c/\pi}\,(1-V_0/V_c) \tag{7}$$

where

$$U_e = x_e/a_c = \left(2+\beta+(1+2\beta)V_0/V_c\right)/3/(1+\beta) \tag{8}$$

$$F(U_e, V_c) = \frac{3.52(1-U_e)}{(1-V_c)^{3/2}} - \frac{4.35-5.28U_e}{(1-V_c)^{1/2}} + \left\{\frac{1.30-0.30U_e^{3/2}}{\left[1-U_e^{2}\right]^{1/2}} + 0.83-1.76\,U_e\right\}\cdot\left\{1-(1-U_e)V_c\right\} \tag{9}$$

$$Z(U_e, V_0/V_c) = \frac{6\,(1.025-0.1\beta)}{1+1.83\,(V_0-0.2)}\left(\frac{V_0}{V_c}\right)^{p}\sqrt{\frac{V_c}{\pi}}\;U_e^{-0.2} \qquad 0.2\le V_0\le 0.8 \tag{10}$$

in which, p = 1.5$(V_0$-0.2) +0.8, when 0.2 ≤ V_0 ≤ 0.6; p = 3(V_0-0.6) +1.4, when 0.6 ≤ V_0 ≤ 0.7; and p = 6 (V_0-0.7) + 1.7, when 0.7 ≤ V_0 ≤ 0.8.

During determining the $\sigma_s(CTOD_c)$, the bilinear softening traction-separation law is adopted as sketched in fig. 6.

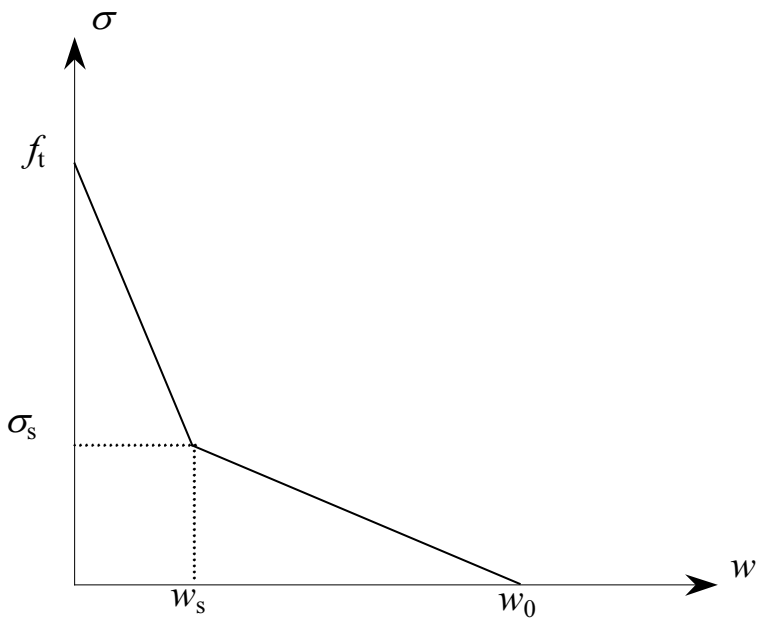

Fig. 6 Illustration of the bilinear softening traction-separation law

The area under the σ-w in fig. 2 is defined as the fracture energy G_F of concrete material (Hillerborg, 1976) . The bilinear softening-traction separation law can be listed as:

$$\begin{aligned} &\sigma = f_t - (f_t - \sigma_s)w / w_s && 0 \le w \le w_s \\ &\sigma = \sigma_s (w_0 - w)/(w_0 - w_s) && w_s \le w \le w_0 \\ &\sigma = 0 && w \ge w_0 \end{aligned} \tag{11}$$

For determining value of the break point (w_s, σ_s) and the crack width w_0, Xu proposed a formulized method based on concrete material's physical meaning (Shilang Xu, 1999)

$$\begin{aligned} w_s &= 0.4\sqrt{\alpha_F}\, G_F / f_t \\ \sigma_s &= \left(2 - 0.4\sqrt{\alpha_F}\right) f_t / \alpha_F \\ w_0 &= \alpha_F G_F / f_t \\ \alpha_F &= \lambda - d_{max}^{0.9}/8 \\ G_F &= (0.0204 + 0.0053 d_{max}^{0.95}/8)(f_c / f_{c0})^{0.7} \\ \lambda &= 10 - \left[f_{ck}/(2 f_{ck0})\right]^{0.7} \end{aligned} \tag{12}$$

where f_t , f_c are the tensile and compressive strength in MPa ; f_{c0}=10MPa ; G_F is the fracture energy in N/mm ; d_{max} is the maximum size of aggregate in mm ; f_{ck} is the characteristic strength representing the concrete grade in MPa; f_{ck0}=10MPa . According to CEB-FIP Model Code 1990 , there is a relation of f_c=f_{ck}+8 MPa . Now it can be seen if concrete grades and the maximum size of aggregate in the concrete are known , all parameters needed in the bilinear softening traction-separation curve can be certainly determined according to equations (12).

In the previous expression (11), one needs to know the $CTOD_c$ corresponding to the peak load to give the correct the evaluation $\sigma_s(CTOD_c)$ needed in equation (7). The following expression is used to determine $CTOD_c$ (Jenq and Shah, 1985):

$$CTOD_c = CMOD_c\left\{(1-a_0/a_c)^2 + (1.018-1.149a_c/D)\left[a_0/a_c - (a_0/a_c)^2\right]\right\}^{1/2} \tag{13}$$

Up to now, the whole procedure for determine the double-K parameters has been completed. The test results from series BM is illustrated in Table 4, also their values are visualized in Fig. 7.

Table 4 The results of double-K parameters from series BM

Nos.of specs.	a_0/D	a_{ck}/D	$CTOD_c$ (mm)	E(Mpa)	K_{Ic}^{c} (Mpam$^{1/2}$)	K_{Ic}^{ini} (Mpam$^{1/2}$)	K_{Ic}^{un} (Mpam$^{1/2}$)
BM102	0.2	0.34	0.026	37950	0.524	1.182	1.706
BM402	0.2	0.298	0.016	36760	0.492	0.747	1.239
BM3402	0.2	0.368	0.035	34255	0.86	0.987	1.847
BM3502	0.2	0.375	0.031	36920	0.807	0.879	1.686
BM3602	0.2	0.286	0.021	29500	0.418	1.007	1.424
Mean			0.026	35080	0.6202	0.9604	1.580
S.D.			0.008	3400	0.1994	0.1614	0.244
C.V.			0.304	0.097	0.3214	0.1680	0.155
BM303	0.3	0.41	0.024	33755	0.48	1.064	1.544
BM2603	0.3	0.406	0.024	31320	0.471	0.984	1.455
BM2703	0.3	0.414	0.029	35015	0.565	1.301	1.866
BM2803	0.3	0.427	0.025	34320	0.513	1.02	1.533
BM2903	0.3	0.434	0.027	33420	0.513	1.043	1.556
BM3003	0.3	0.448	0.026	36840	0.564	0.975	1.539
Mean			0.026	34110	0.51767	1.0645	1.582
S.D.			0.002	1830	0.0401	0.1207	0.144
C.V.			0.076	0.054	0.0774	0.1134	0.091
BM705	0.5	0.553	0.018	32790	0.344	1.313	1.658
BM805	0.5	0.567	0.017	29322	0.405	0.835	1.24
BM1205	0.5	0.626	0.020	41870	0.614	0.767	1.381
BM1305	0.5	0.642	0.030	38010	0.736	0.936	1.672
BM1505	0.5	0.582	0.017	42020	0.464	1.069	1.532
BM2005	0.5	0.566	0.017	37140	0.405	1.098	1.503
Mean			0.020	36860	0.4947	1.0030	1.498
S.D.			0.005	5030	0.1498	0.1989	0.166
C.V.			0.247	0.1365	0.3028	0.1983	0.111
BM1406	0.6	0.738	0.022	36170	0.728	0.486	1.214
BM1806	0.6	0.695	0.020	39270	0.523	0.994	1.517
BM1906	0.6	0.719	0.013	43485	0.728	0.257	0.985
Mean			0.019	39640	0.6597	0.5790	1.239
S.D.			0.005	3670	0.1184	0.3772	0.267
C.V.			0.255	0.093	0.1794	0.6515	0.215

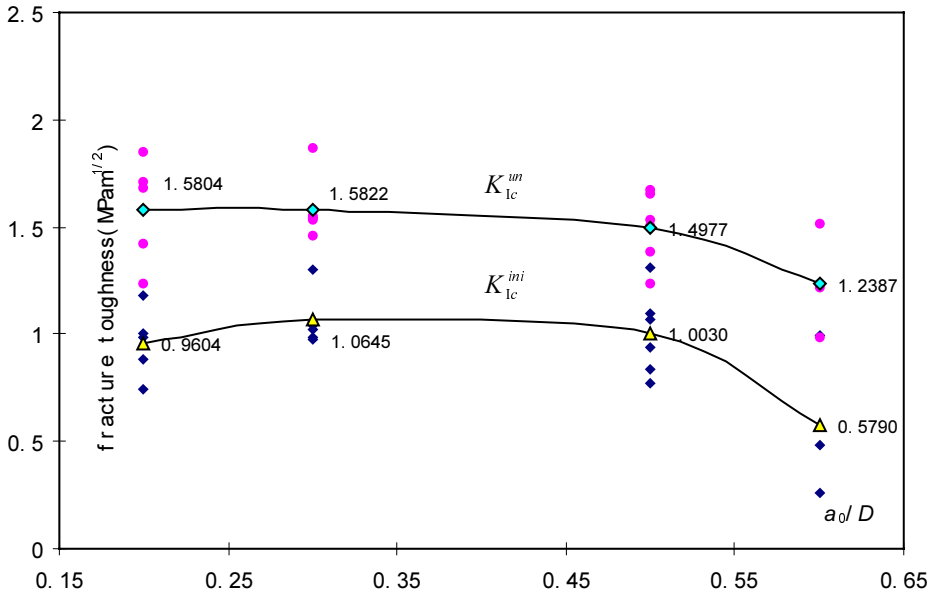

Fig. 7 The values of K_{Ic}^{ini} and K_{Ic}^{un} measured from series BM

THE CALCULATIONS EQUATIONS FOR WS

WS specimens are gaining more and more attentions because of its nonconsideration of the specimen weight during the determination of fracture parameters. They are widely used now to measure the fracture parameter of concrete materials (Xu et al., 1991; Brühwiler and Wittmann, 1990).

For WS specimens, the same procedure is conducted to get the comparison of the effective crack length a_{ck} in double- and a_{cp} in the TPFM, and the double-K fracture toughness K_{Ic}^{ini} and K_{Ic}^{un} can also be obtained. The following briefed the expression used in the calculation.

The formula to determine the fracture parameters of wedge splitting specimens are the same to the CT (compact tension) due to the geometry and the loading condition like each other. During the test, the veritcal load P_v and the *CMOD* are recorded , this is not like the CT in which the P_h and *CMOD* on the load line are directly recorded. But certain relation is existed when taking the wedge angle α (as illustrated in Fig. 2(b)) into account:

$$P_h = P_v/(2tg\alpha) \tag{14}$$

in this report, α is equal to 15^0.

For the geometry of test specimens WS used in this report basically satisfy the standard CT-specimen recommended by ASTM standard E-399-72 (1972), the formula for determining the Young's modulus can be listed as (Murakami, 1987):

$$E = V_2(\alpha_0)/BC_{ih} \tag{15}$$

where

$$V_2(\alpha_0) = \left(\frac{1+\alpha_0}{1-\alpha_0}\right)^2 (2.163 + 12.219\alpha_0 - 20.065\alpha_0^{\,2} - 0.9925\alpha_0^{\,3} + 20.609\alpha_0^{\,4} - 9.9314\alpha_0^{\,5}) \tag{16}$$

in which

$\alpha_0 = (a_0+H_0)/(D+H_0)$;

C_{ih} = the initial compliance of P_h-*CMOD*, equal to $2\mathrm{tg}\alpha C_{iv}$, C_{iv} is the initial compliance of P_v-*CMOD*

B = the thickness of WS specimens;

H_0 = thickness of clip gauge holder.

This step for calculating the Young's modulus is the same for both the TPFM and the double-*K* criterion.

While for the determination of the effective crack length, attentions may be paid to employment of the compliance of P_h-*CMOD* curve or P_v-*CMOD* curve

$$E = V_2(\alpha_{ck})/BC_{sh} \tag{17}$$

where

$\alpha_{ck} = (a_{ck}+H_0)/(D+H_0)$;

C_{sh} = the scant compliance from P_h-*CMOD* curve , equal to $CMOD_c/P_{maxh}$, or equal to $2\mathrm{tg}\alpha C_{sv}$, C_{sv} is the scant compliance from P_v-*CMOD* curve.

For the TPFM, the effective crack length a_{cp} is using the same expression except the use of different compliance, replace the C_{sh} in equation (17) with C_{uh}, or C_{sv} with C_{uv} which is the unloading compliance of P_v-*CMOD* curve of 95% peak load. The calculation results are listed in Table 5.

*Table 5 The comparison of the TPFM and the double-*K *in terms of effective crack length for WS specimens*

No.	a_0/D	C_{iv}x10^{-3} (mm/KN)	C_{sv}x10^{-3} (mm/KN)	C_{uv}x10^{-3} (mm/KN)	E(Mpa)	a_{ck}/D	a_{cp}/D
1	WS102	2.796	6.613	6.436	35315	0.411	0.410
2	WS2902	2.832	6.704	5.618	34860	0.409	0.378
3	WS2103	4.823	9.918	8.212	36150	0.498	0.466
4	WS2203	4.760	11.551	10.591	36625	0.530	0.520
5	WS2303	4.814	10.771	10.852	36220	0.513	0.523
6	WS2403	4.257	9.959	9.113	40955	0.523	0.513
7	WS2703	4.768	10.298	9.589	36560	0.507	0.500
8	WS704	7.792	15.179	15.751	38980	0.589	0.604
9	WS804	5.183	13.226	12.223	58600	0.633	0.630
10	WS904	9.083	20.858	19.319	33440	0.615	0.613
11	WS1004	9.756	21.910	19.185	31130	0.612	0.600
12	WS1104	8.272	18.735	17.271	36720	0.613	0.610
13	WS1205	15.236	26.259	24.191	36660	0.660	0.662
14	WS1305	15.277	31.707	25.849	36560	0.687	0.672
15	WS1405	15.475	30.403	24.470	36090	0.681	0.662
16	WS1505	15.284	37.711	33.001	36540	0.709	0.705
17	WS1605	14.891	33.271	28.320	37505	0.697	0.688
18	WS1705	15.549	32.558	23.914	35920	0.690	0.658
19	WS2005	15.512	26.132	22.671	36005	0.659	0.650
20	WS2506	33.551	77.162	53.078	36220	0.782	0.760
21	WS2606	33.989	88.081	71.736	35760	0.790	0.789
22	WS3006	32.999	67.710	55.335	36830	0.771	0.766
23	WS3106	33.592	54.123	42.759	36180	0.744	0.736

While for the double-K fracture toughness K_{Ic}^{ini} and K_{Ic}^{un} in WS specimens, the same procedure is samely carried out as series BM as presented above, and the calculated results are listed in Table 6 and Fig. 8.

Table 6 The results of double-K parameters from series WS

Nos.of specs.	a_0/D	a_{ck}/D	$CTOD_c$ (mm)	E(MPa)	K_{Ic}^{c} (MPam$^{1/2}$)	K_{Ic}^{ini} (MPam$^{1/2}$)	K_{Ic}^{un} (MPam$^{1/2}$)
WS1803	0.353	0.514	0.028	35740	0.787	0.55	1.337
WS2103	0.353	0.498	0.029	36150	0.712	0.794	1.506
WS2203	0.353	0.53	0.031	36625	0.8	0.612	1.412
WS2303	0.353	0.513	0.025	36220	0.826	0.374	1.2
WS2403	0.353	0.523	0.027	40955	0.83	0.588	1.419
WS2703	0.353	0.507	0.028	36560	0.762	0.629	1.391
WS2803	0.353	0.529	0.031	36660	0.786	0.655	1.441
Mean			0.029	36990	0.7861	0.6003	1.387
S.D.			0.002	1780	0.0404	0.1261	0.097
C.V.			0.079	0.048	0.0514	0.2100	0.07
WS604	0.471	0.581	0.018	35430	0.739	0.313	1.053
WS704	0.471	0.589	0.022	38980	0.73	0.623	1.354
WS904	0.471	0.615	0.026	33440	0.793	0.435	1.228
WS1004	0.471	0.612	0.028	31130	0.751	0.479	1.23
WS1104	0.471	0.613	0.024	36720	0.812	0.46	1.271
Mean			0.024	35140	0.7650	0.4620	1.227
S.D.			0.004	3010	0.0357	0.1108	0.11
C.V.			0.163	0.086	0.0466	0.2399	0.09
WS1205	0.588	0.66	0.012	36660	0.622	0.33	0.953
WS1305	0.588	0.687	0.018	36560	0.738	0.415	1.153
WS1405	0.588	0.681	0.019	36090	0.688	0.564	1.252
WS1505	0.588	0.709	0.021	36540	0.84	0.351	1.191
WS1605	0.588	0.697	0.020	37510	0.777	0.469	1.245
WS1705	0.588	0.69	0.021	35920	0.716	0.593	1.309
ws1905	0.588	0.667	0.016	36375	0.631	0.544	1.175
ws2005	0.588	0.659	0.014	36005	0.598	0.502	1.099
Mean			0.017	36460	0.7013	0.4710	1.172
S.D.			0.003	506	0.0833	0.0980	0.11
C.V.			0.187	0.014	0.1188	0.2081	0.094
WS2506	0.706	0.782	0.017	36220	0.675	0.593	1.268
WS2606	0.706	0.79	0.016	35760	0.753	0.368	1.12
WS3006	0.706	0.771	0.014	36830	0.614	0.573	1.186
WS3106	0.706	0.744	0.008	36180	0.445	0.497	0.942
Mean			0.014	36250	0.6218	0.5078	1.129

Continuation of Table 6

S.D.			0.004	440	0.1308	0.1019	0.139
C.V.			0.286	0.012	0.2104	0.2008	0.123

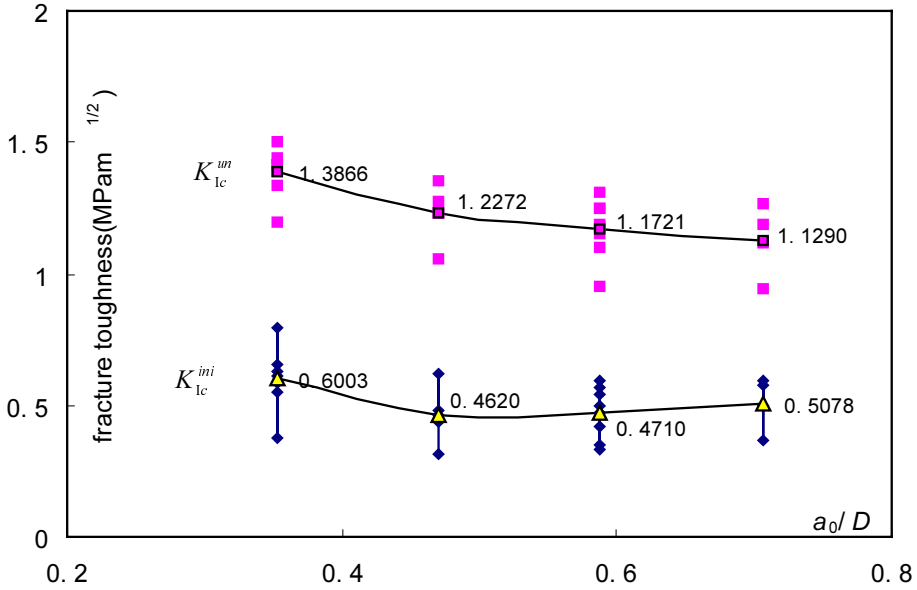

Fig. 8 The values of K_{Ic}^{ini} *and* K_{Ic}^{un} *measured from series WS*

4 CONCLUSION

For decades, the nonlinearity behavior of *P-CMOD* curve observed in testing three-point beams has been one of the study focuses in the concrete fracture mechanics. Based on the different explanation and hypothesis about this phenomenon, many models depicting the concrete fracture characteristics have been presented. In this report, a detailed comparison is made between the Two Parameter Fracture Model (TPFM), typical in the existing literature, and the double-*K* fracture criterion proposed in recent years.

There is a growing recognition that the fracture process in the concrete structures consists of three apparent stages: the crack initiation, stable propagation and the unstable propagation. And it is widely accepted that the nonlinearity of *P-CMOD* curve is mainly associated with the FPZ. In the calculation of the effective crack length a_c, it should includes both the unrecoverable deformation $CMOD^*$ and one part of the elastic deformation $CMOD^e_n$, the difference between unloading compliance C_u. and the initial compliance C_i. While in the TPFM, in

order to employ the LEFM, only the latter part, the elastic $CMOD^{e}_{n}$ is taking into account, which will obviously underrate the true value of a_c .And in the tests, it is not so easy to control the unloading procedure in the peak load. To equalizing this deficiency, RILEM proposed to adopt the unloading compliance C_u after 95% peak load as one means of compensation. From Table 3 and Table 5, it can be seen that the value of the effective crack length a_c differs very marginally from the double-*K* fracture criterion. So it can tell that this compensatory method is feasible.

Comparing with the TPFM, the double-*K* fracture criterion covers more completely in describing the concrete fracture process: in addition to the unstable fracture toughness K_{Ic}^{un} , similar to the K_{Ic}^{s} in the TPFM, representing the onset of the unstable crack propagation, the initial fracture toughness K_{Ic}^{ini} is also introduced to describing the commencement of stable crack growth, and they are correlated by the cohesive forces acting on the FPZ.

Besides the more established in the theory concept, the double-*K* criterion is more practical in the applicability. In the TPFM, to obtain the unloading compliance C_u, a closed-loop testing system is required to achieve the stable unloading procedure. It is also shown in this report that the unloading procedure is uneasy to be accessed. Otherwise in the double-*K* model, for the determining the fracture parameters, such as a_c, only a monotonic loading is needed to carried out, without unloading procedure.

From the comparison between the TPFM and the double-*K* fracture criterion, it can be said that the double-*K* fracture criterion is more complete in the theory concept, more simple and convenient in the testing method. For most common materials and structural labs, this model is practical.

ACKNOWLEDGEMENT

This paper is supported by the National Key Basic Research and Development Program (973 Program) No. 2002CB412709.

REFERENCE

[1] ASTM Standard E399-72 (1972). Standard Method of Test for Plane-Strain Fracture Toughness of Metallic Materials. Annual Book of ASTM Standard.

[2] Bazant, Z. P. and Oh, B. H. (1983). Crack band theory for fracture of concrete. **RILEM. Materials and Structures 16(93)**, 155-177.

[3] Bazant, Z. P., Kim, J.K. and Pfeiffer, P.A. (1986). Determination of fracture properties from size effect tests. **Journal of Structural Engineering. ASCE, 112 (2)**, 289-307.

[4] Bazant, Z. P. (1996). Analysis of work-of-fracture method for measuring fracture energy of concrete. **Journal of Engineering Mechanics ASCE 122**, 138-144.

[5] Brühwiler, E. and Wittmann, F. H. (1990). The wedge splitting test, a new method of performing stable fracture mechanics test. **Engineering Fracture Mechanics 35 (1-3),** 117-125.

[6] CEB-Comite Euro-International du Beton-EB-FIP Model Code 1990 (1993), Bulletin D'Information No. 2132/214, Lausanne.

[7] Hillerborg, A., Modeer, M and Petersson, P. E. (1976). Analysis of crack formation and crack growth in concrete by means of fracture mechanics and finite elements. **Cement and Concrete Research 6**, 773-782.

[8] Jeng, Y. S. and Shah, S. P. (1985). Two parameter fracture model for concrete. **Journal of Engineering Mechanics, ASCE, 111 (10)**, 1227-1241.

[9] Karihaloo, B. L. and Nallathambi, P. (1990). Effective crack model for the determination of fracture toughness (K_{Ic}^{s}) of concrete. **Engineering Fracture Mechanics 35 (4/5),** 637-645.

[10] Murakami (Editor-in-Chief) (1987). Stress Intensity Factors Handbook. Pergamon Press, London.

[11] Refai, T. M. E. and Swartz, W. E. (1987). Fracture Behaviour of Concrete Beams in Three-Point Bending considering the influence of Size-Effects. Report No. 190, Engineering Experiments Station, Kansas State University.

[12] RILEM Technical Committee 89-FMT (1990). Determination of fracture parameters (K_{Ic}^{s} and $CTOD_c$) of plain concrete using three-point bend tests, proposed IRLEM draft recommendations. **RILEM. Materials and Structures 23 (138),** 457-460.

[13] Tada, H., Paris, P. C. and Irwin, G. R. (1985). The Stress Analysis of Cracks Handbook. Paris Productions Incorporated, St. Louis, Missouri, USA.

[14] Xu Shilang and Reinhardt, H. W. (1999a). Determination of double-*K* criterion for crack propagation in quasi-brittle fracture: Part I-Experimental investigation of crack propagation. **International Journal of Fracture, 98 (2)**, 111-149.

[15] Xu Shilang and Reinhardt, H. W. (1999b). Determination of double-*K* criterion for crack propagation in quasi-brittle fracture: Part II-Analytical evaluation and practical measuring methods for three-point bending notched beams. **International Journal of Fracture, 98 (2)**, 151-177.

[16] Xu, Shilang and Hans W. Reinhardt (1999c). Determination of Double-K Criterion for Crack Propagation in Quasi-Brittle Materials, part III: Compact Tension Specimens and Wedge Splitting Specimens. **International Journal of Fracture, 98 (2)**, 179-193.

[17] Xu Shilang and Reinhardt, H. W. (2000). A simplified method for determining double-*K* fracture parameters for three-point bending tests. **International Journal of Fracture, 104 (2)**, 181-208.

[18] Xu Shilang (1999). Determination of parameters in the bilinear, Reinhardt's non-linear and exponentially non-linear softening curves and their physical meanings. **Werkstoffe und Werkstoffprüfung im Bauwesen**, Hamburg, Libri BOD, 410-424.

[19] Zhao, G., Jiao H. and Xu, S. (1991). Study on fracture behaviour with wedge splitting test method. **Fracture Processes in Concrete, Rock and Ceramics** (Edited by van Mier et al.), E & F.N. Spon, London, 789-798.